

# EVALUATION OF FLOOD REGULATION ROLE OF PADDIES IN THE LOWER MEKONG RIVER BASIN USING A 2D FLOOD SIMULATION MODEL

Pham Thanh HAI<sup>1</sup>, Takao MASUMOTO<sup>2</sup> and Katsuyuki SHIMIZU<sup>3</sup>

<sup>1</sup>Member of JSCE, Dr. of Eng., Postdoctoral Researcher, National Institute for Rural Engineering (2-1-6, Kan-nondai, Tsukuba, Ibaraki, 305-8609, Japan)

<sup>2</sup>Member of JSCE, Dr. of Agr., Head of Hydrology and Water Resources Lab., National Institute for Rural Engineering (2-1-6, Kan-nondai, Tsukuba, Ibaraki, 305-8609, Japan)

<sup>3</sup>Dr. of Agr., Postdoctoral Researcher, National Institute for Rural Engineering (2-1-6, Kan-nondai, Tsukuba, Ibaraki, 305-8609, Japan)

From the viewpoint of watershed management, paddy areas are regarded as having important functions beyond their role in food production; these include flood regulation, fostering of water resources, and prevention of soil erosion. These functions are commonly found in low-lying paddy areas such as in Japan, Cambodia, Vietnam, and other countries, where the levels of development of paddy irrigation are quite different. In this study, a flood inundation model, which covers floodplains of the Mekong River from Kratie in Cambodia to near the Vietnamese border, was developed by using the FEM technique with 2-D shallow water equations. The model was applied to the water flows over the years 1996 through 2003. Main roads, dikes, colmatages, and waterway-opening works in the study area, which enable water to be stored, were taken into account in the simulation. The flood regulation function of paddy fields in the study area was then assessed, using the results of the model simulation and land-use data. Namely, the volume of flooded water on paddies was estimated in order to evaluate the impact of flood storage by paddies on floods and water use. The results showed that about one-fifth of the total flood volume is stored on paddies in and around Tonle Sap Lake, and rice cultivation starting after the flood waters recede.

**Key Words :** 2-D FEM, regulation functional role of paddies, flood process, Mekong River basin, Tonle Sap Lake and its environs

## 1. INTRODUCTION

A unique feature of the flow in and around Tonle Sap Lake and its environs in the Mekong River system is the existence of reverse flows into the lake from the Mekong River. This phenomenon occurs annually; that is, in May/June, the water from the main Mekong River flows down to the lower Mekong and Bassac rivers, and at the same time flows upstream into Tonle Sap Lake. In September/October, when the water level of Tonle Sap Lake is higher than that of the Mekong River, this stored water starts to drain into the lower Mekong and Bassac rivers<sup>1)</sup>. This natural mechanism provides a unique and important balance to the Mekong River downstream of the lake and

ensures a fresh water flow into the Mekong Delta in Vietnam during the dry season, protecting the rich agricultural lands of the delta from salt water intrusion from the South China Sea. In order to assess this unique feature of flooding processes, a two-dimensional finite element method (FEM) simulation model was developed using full terms of depth-averaged shallow water motion equations. Such models are capable of addressing the geometric complexity usually found in topography as well as at the boundaries of the study area. The results of the model simulation and land-use data were used to evaluate the flood prevention function of paddies in Tonle Sap Lake and its environs. That is, the volume of flooded water on paddies was estimated in order to evaluate the impact of

non-irrigated paddies on floods and water use.

## 2. MODEL DESCRIPTION

### (1) Flow equations

The simulation model is based on an explicit two-step, finite element method that is capable of predicting water depth, mean velocities in the vertical direction, and the positions of wet and dry areas during water flow propagation. The formulation of flow processes can be described as two-dimensional St. Venant equations for shallow water problems, as follows:

$$\dot{H} + H_{,i}u_i + Hu_{i,i} = 0 \quad (2.1)$$

$$\begin{aligned} \dot{u}_i + u_j u_{i,j} - \varepsilon(u_{j,i} + u_{i,j})_{,j} + g(H+z)_{,i} + \\ + \frac{gn^2 \sqrt{u_k u_k}}{H^{4/3}} u_i - \frac{K|W|W_i}{H} + fu_i = 0 \end{aligned} \quad (2.2)$$

where  $i$  ( $=1, 2$ ) or  $j$  ( $=1, 2$ ) are subscript for horizontal coordinates ( $=x, y$ ) and  $t$  is the time. Differentiations with respect to  $(x, y)$  and  $t$  are denoted by subscripted comma and superscripted dot, respectively.  $H(x, y, t)$  is water depth;  $u_i(x, y, t)$  is the depth averaged velocities;  $\varepsilon$  is eddy viscosity coefficient;  $g$  is gravitational acceleration;  $z$  is bed elevation;  $n$  is the Manning coefficient of roughness;  $K$  is wind stress coefficient;  $W$  is wind velocity; and  $f$  is Coriolis parameter.

### (2) Conversion of DEM data and generation of finite element meshes

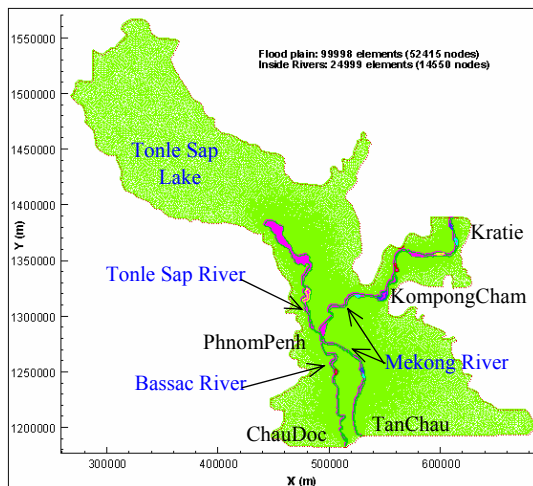


Fig.1 Generated FEM meshes of the study area.

The topographic data used in the model is a 100m x 100m grid Digital Elevation Model (DEM) map (provided by the Mekong River Commission,

or MRC), which covers the Mekong flood-plain from Kratie to the center of the Mekong Delta in Vietnam. For the DEM map, ERDAS Imagine software was used to convert raster image data to an ASCII data set. The selected study area, in which the necessary data was converted, covers floodplains of the Mekong River from Kratie in Cambodia to Tan-Chau in Vietnam, the Bassac River down to Chau-Doc in Vietnam, the Tonle Sap River and Tonle Sap Lake. These converted data were used in generating the mesh and interpolating bed elevations at FEM nodes.

In this study, Mesh-Generator software was used to generate unstructured triangular FEM meshes. To create flood-plain and river boundaries, we extracted outer points from converted data of flood-plain and main river domains; these flood-plain and river boundaries were used as external and internal boundaries in mesh generation. Where rivers are meandering, the boundary node distribution was modified so as to result in a smoother mesh. In order to generate refined FEM meshes, mesh sizes were selected following consideration of the topography, the scale of the study area and mesh smoothing conditions; mesh size in the flood-plain area was from 2500 m to 5000 m, and from 200 m to 450 m inside the main river elements. The final generated meshes of the entire study area are shown in **Fig. 1**. The meshes have total of 124,997 elements and 62,965 nodes. The bed elevations of grids in the DEM data were used to interpolate the elevations of FEM nodes in the flood-plain domain, while more precise and newly updated bathymetry data of the main rivers were utilized to interpolate the elevations of FEM nodes in the main river domain. In addition, a bilinear interpolation algorithm was used to interpolate elevations of FEM nodes in the flood-plain area, and a nearest-point interpolation algorithm was applied for interpolating elevations of FEM nodes in the main river areas.

### (3) Solution of the flooding processes by FEM

The weighted-residual of the standard Galerkin FEM was applied to the 2-D shallow water equations Eqs. (2.1) and (2.2) for spatial discretization, and the selective lumping two-step explicit FEM was employed for numerical integration in time, in a method proposed by Kawahara *et al.*<sup>2)</sup>. In the simulation, a selective lumping parameter,  $e$ , was used to reduce the numerical damping effect and to adjust the numerical stability. We chose  $e=0.85\sim 0.9$ . A time increment,  $\Delta t=(1\sim 10)\text{sec}$ , was used in the calculation as the time stepping scheme employed should yield a stable Courant number.  $n_R=0.02$  and

$n_f=0.025$  of Manning roughness coefficients were used for main rivers and floodplains, respectively.

The model was coded so that initial conditions could vary: it could either assign values to  $u$ ,  $v$ ,  $H$  variables, with a starting velocity of zero ( $u=0$ ,  $v=0$ ) and a linear water surface slope based on observed water level data, or use the results of the previous solution. As for boundary conditions, slip conditions were imposed along land boundaries so that normal velocities of nodes belonging to land boundaries were set to zero. The observed (or calculated) discharges of 12 tributaries around Tonle Sap Lake were set up as constantly wet nodes; during the dry season these are inflow boundaries, located at the lake's water edge. Upstream inflow conditions were specified by measured water levels as a function of time at the Kratie water level gauge, while levels at the Tan Chau and Chau Doc water level gauges were used to specify downstream outflow conditions. The moving boundary problem was addressed by applying a threshold technique, in which a thin water depth was reset in dry nodes of all moving boundary elements each time. In order to avoid artificial water flow from wet to dry nodes numerically, water depths of moving boundary dry nodes were kept as minus values ( $H<0$ ). This approach handled the problem of moving boundaries well due to the study area's wetting/drying cycle. More details of this approach are described in Pham *et al.*<sup>3)</sup>

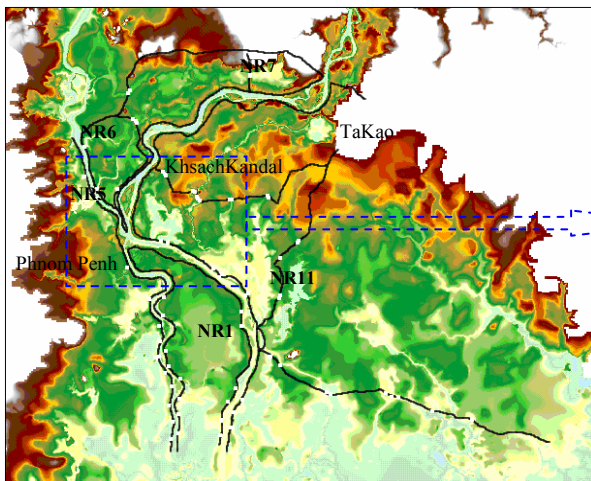


**Fig.2** Selected roads, dikes and road-opening works in the model simulation.

### 3. ASSIGNING ELEVATIONS OF MAIN ROADS, DIKES AND ROAD-OPENING WORKS TO FEM NODES

The elevations of those construction works that have a significant influence on flow regimes in the

study area were assigned to FEM nodes in the model simulation. Construction works were selected based on the “Road Opening Survey” report of MRC<sup>4)</sup> and other available data, and included National-Road (NR) 1 from Phnom Penh to the Vietnam border; NR5, NR6, and NR7; a local road on the left bank of the Mekong River, from Khsach Kandal to the junction with NR11 at TaKao; dikes on both sides of the Mekong River from KomPong Cham to near Tan Chau; dikes of the Tonle Sap River from Phnom Penh to Prek Dam; dikes on both sides of the Bassac River, from Phnom Penh to near Chau Doc; and main road-opening works located on the selected roads and dikes (**Fig. 2**). ArcGIS (ESRI) was used to convert the polyline shape data of the selected roads, dikes and road-opening works to point data. Coordinates of these points were used to find the FEM nodes closest to the points, and the elevations of the selected roads, dikes and road-opening works were then assigned to those FEM nodes (**Fig. 3**).

### 4. APPLICATION FOR EVALUATING FLOOD REGULATION ROLE OF PADDIES

#### (1) Simulation results

After applying the methods and parameters mentioned above, the following simulation results were obtained. Simulated results of water depth and

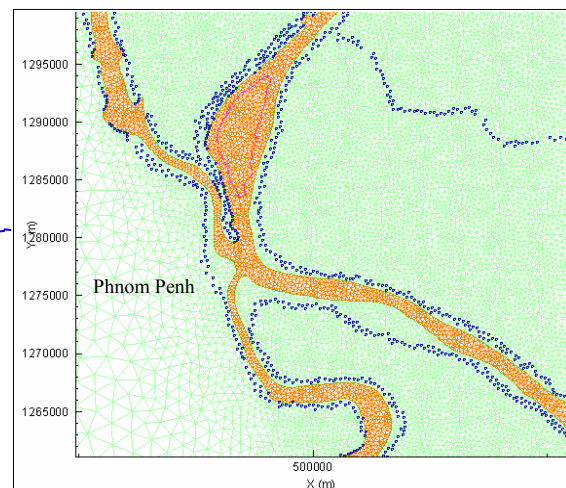


**Fig.3** FEM nodes in which elevations of the selected roads, dikes and road-opening work are assigned.

flood extents of year 2000 and on 9 October 2003 are shown in **Fig. 4**. The simulated flow-fields in inundated areas around the confluence near Phnom Penh on 1 September 2000 are shown in **Fig. 5**. Model results described the real features of the area's flood flows; e.g., in the annual monsoonal

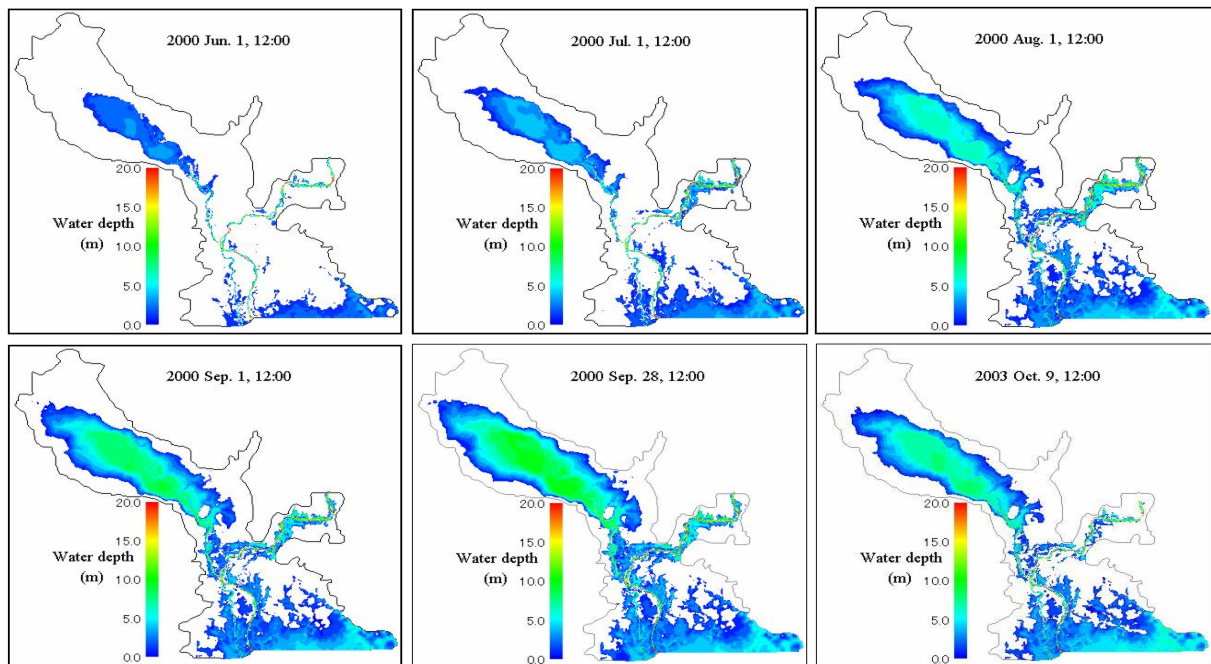


**Fig.4** Simulated results of inundation processes on the 1st days of June, July, August, September Year 2000, and maximum flood extent on Sep. 28th of year 2000 and Oct. 9th of year 2003.

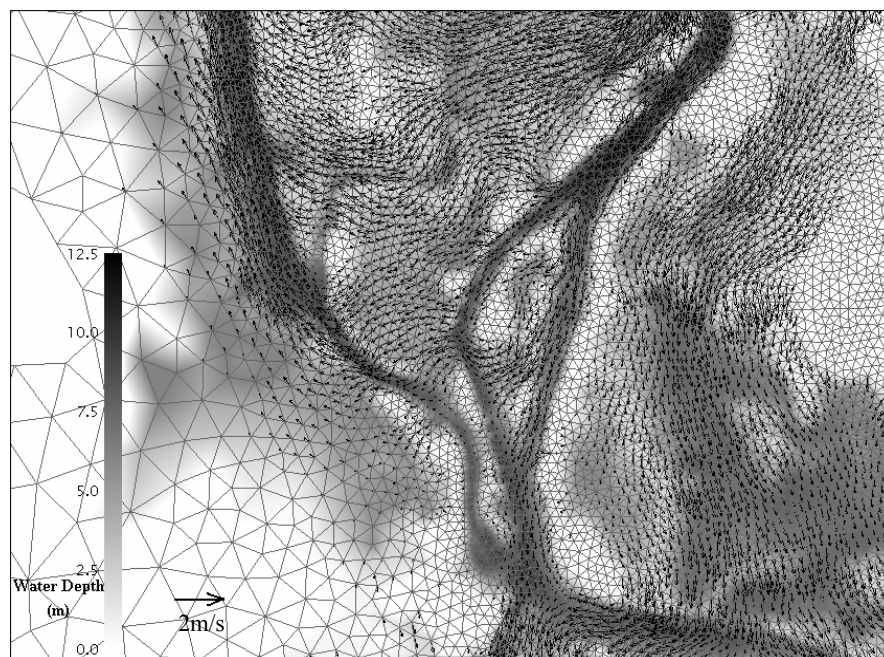


**Fig.5** Simulated flow-field at the confluence of the Tonle Sap & Mekong Rivers on Sep. 1<sup>st</sup>, Year 2000.

wet season (from June to October), Mekong River floodwaters flow downstream to the lower Mekong and Bassac rivers. At the same time, part of this high water reverses its flow and travels upstream, into the Tonle Sap River and towards Tonle Sap Lake, where the water level is lower. This reverse water flow increases the size of the lake. **Fig. 5** describes these features of the rising stage of the flood flow during the wet season in the study area. Simulated water levels at Kompong Luong in Tonle

Sap Lake during wet season were 2.4 m, 4.3 m, 7.4 m, 8.5 m, and 9.8 m, corresponding to the first day of June, July, August, September, and October 2000, respectively. The simulated results reproduced the inundation processes occurring during the year: At the beginning of wet season (June), water was flowing only in the main rivers; at the onset of the flood (July), flood water spilled out gradually to adjacent areas, expanding the flood plain on both sides of the main rivers. Simulated

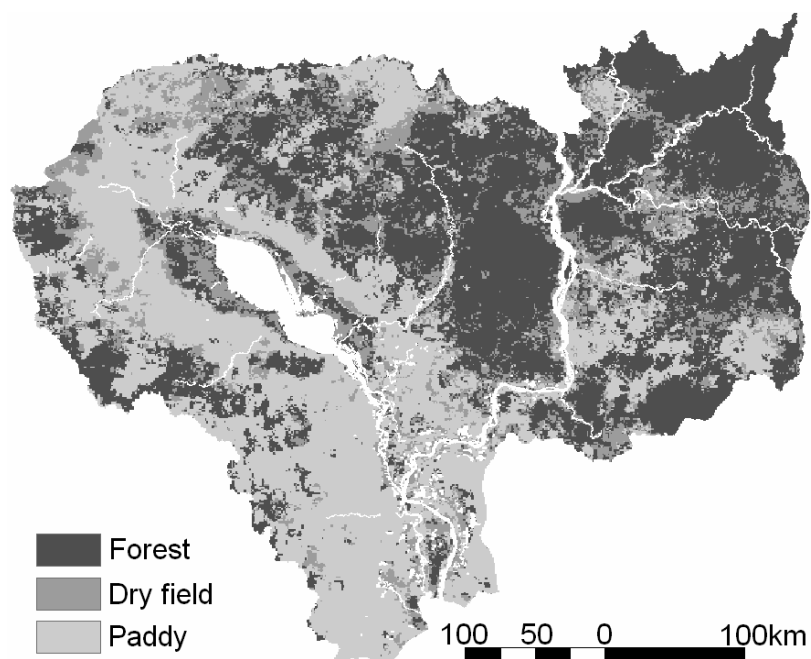


**Fig.6** Land use in and around Tonle Sap Lake (Source: USGS).

**Table 1** Types of rice fields and rice production in Cambodia.

Type of crop pattern of paddies	Area (km <sup>2</sup> )						Rice Production (ton)	Rice Yield (ton/ha)
	Early	Medium	Late	Floating	Upland	Total		
	3,589	7,647	5,657	960	359	18,212	2,915,900	1.71

Source: Agricultural Statistics 2002 Department of Planning and Statistics, MAFF (Cambodia)

**Table 2** Estimated flood inundation area and volume for years 2000 and 2003.

Year	Flooded area of paddies (km <sup>2</sup> )	Flooded volume in paddies (10 <sup>9</sup> m <sup>3</sup> )	Ratio of flooded volume in paddies to the total (%)
2000 as a recent largest flood year	12,249	21.914	22.4
2003 as a recent drought year	5,527	8.171	15.1

water levels were compared with observed hydrographs at five points and maximum flood extents. The calculated water levels were a little bit lower than the observed ones.

## (2) Estimation of flooded water on paddies

### a) Agricultural lands in Cambodia

Agricultural land use in and around Tonle Sap Lake is classified roughly as paddies and dry fields. **Fig. 6** shows land use in Cambodia with the simple classifications of forest, dry fields, and paddies. The grid size of the digital map is 1 km. There are various types of paddy rice-cropping patterns (**Table 1**). Rice maturity types include early, medium, and late, and are related to annual planting stages that vary according to the availability of water and the height of flood levels. Areas in and

around Tonle Sap Lake are used in particular for rice that is planted as the flood waters recede<sup>5)</sup>.

### b) Estimation of inundation volume on paddies

In order to evaluate the role of agricultural lands in flood protection and agricultural water use, we estimated the volume of flooded water on paddies. The estimation was carried out by summing the height of floods (**Fig. 4** shows one example) in accordance with all grid-cells of paddies and dry fields (**Fig. 6**). **Fig. 4** shows the maximum inundated area and water depth in years 2000 and 2003, respectively. The years 2000 and 2003 are representative of the most significant recent flood and drought years, respectively.

**Table 2** shows the calculated results for the flooded area of paddies, the flooded volume in the

paddies, and the ratio of the flooded volume in the paddies to the total flooded volume. Using the year 2000 flood as an example, about 42% (12,249 km<sup>2</sup>/29,280 km<sup>2</sup>) of paddies in Cambodia were affected, and it was estimated that paddies apparently stored 22.4% of the entire flooded volume in and around Tonle Sap Lake and environs. Even for the recent smallest flood (in 2003), the flooded volume on the paddies accounts for 15.1% of total storage (based on apparent value at the peak). In total, the ratio of flooded areas to the total paddy area in Cambodia varied from 30% (2003) to 42% (2000). The ratio of the flooded volume on paddies to the total flood was about 19%. Hence, we can say that roughly one-fifth of the total flood volume was stored on paddies in and around Tonle Sap Lake. In addition to the estimated flooded volume on paddies, flooding areas and the volume on dry fields were also calculated. The results of these estimates show that dry fields in and around Tonle Sap Lake were also flooded, at the same or greater volume as paddies, while the size of the flooded areas/volumes on dry fields was not large compared with paddies in the colmatage area.

## 5. DISCUSSION ON THE RESULTS AND CONCLUSIONS

In this study, a 2D-FEM model with refined, unstructured-triangular mesh was developed that was well matched to the topographical geometric complexity and the boundaries of the study area. Main roads, dikes and road-opening works affect flow regimes, and were therefore introduced in the simulation. As a result, this simulation model can describe the expansion and shrinking processes of flood plains on both sides of main rivers accurately and in detail, especially in the case of flood plains downstream of Phnom Penh, and on the left bank of the main Mekong River, which existing one- and two-dimensional models of the study area could not do. The model simulations showed the real inundation processes occurring in the study area. In particular, when the discharge exceeds the flow capacity of the main river channel, as is the case in the Mekong and Tonle Sap rivers, the excess water was stored in the lower part of the basin as the flood water rose above the dikes. Moreover, when water level of the Mekong River is higher than that of Tonle Sap Lake, excessive water flows into the lake. A significant feature of land use in the flooded areas of Tonle Sap Lake and its environs are paddies, which extend along both the main river channels and the lake. These paddies serve to store floodwaters; as a result, they could help reduce the risk of flooding in major rivers downstream,

especially in areas from Phnom Penh in Cambodia to the Mekong Delta in Vietnam.

In addition, storage areas that are formed by dikes in paddy areas not only protect the urban areas from floods, but also supply irrigation water for downstream paddies. As demonstrated by the analysis for years 2000 and 2003, excess flood water can be stored in many locations and then released gradually, enabling downstream farmers to utilize the water. In the Mekong River drainage system, the relationship between the maximum river discharge and flood-storage capacity is fixed; other places will suffer from flood damage unless capacity to store flood water still exists in the Tonle Sap and its environs.

Finally, the model was applied to inundation processes in the floodplains of Tonle Sap Lake and its environs, where hydro-meteorological data had been missing for a long time due to the civil war in the area. Then, the simulated results on this area produced a lot of hydrologic information to us. DEM topographic data was used, as these are commonly available for many lowland floodplain areas. Therefore, the model can be applied to other river basins.

**ACKNOWLEDGMENT:** The authors would like to acknowledge the grant supported from the Revolutionary Research Project "Coexistence of People, Nature and the Earth (RR2002)" of the Ministry of Education, Culture, Sport, Science and Technology (MEXT) of Japan. Our thanks also go to the Technical Support Division of the Mekong River Commission Secretariat (MRCS) for sharing topography and hydrologic data, which are used in this study.

## REFERENCES

- 1) Masumoto, T.: Modelling of multi-functional hydrological roles of Tonle Sap Lake and its vicinities, *Hyd. Env. Model. in the Mekong Basin*, MRC, pp.181-192, 2000.
- 2) Kawahara, M. and Umetsu, T.: Finite element method for moving boundary problems in river flow, *Int. Jour. for Numerical Methods in Fluids*, Vol. 6, pp.365-386, 1986.
- 3) Pham, T. Hai, Masumoto, T. and Shimizu, K.: Development of a 2D-FEM simulation model for flood flows in Tonle Sap Lake and its environs. *Proc. of Advances in Integrated Mekong R. Manag.*, pp.339-346, 2004.
- 4) Mekong River Commission: Consolidation of hydro-meteorological data and multi-functional hydrologic roles of Tonle Sap Lake and its vicinities, 2003.
- 5) Masumoto, T. Shimizu, K. Pham, T. Hai: Impact of paddy irrigation levels on floods and water use in the Mekong River basin, *Proc. of Advances in Integrated Mekong R. Manag.*, pp.158-165, 2004.

(Received September 30, 2005)